Peter HEYES*, Xiaobin LIN*, Andrzej BUCZYŃSKI**,
Mike BROWN***

Application of Biaxial Plasticity and Damage Modelling to the Life Prediction and Testing of Automotive Components

* nCode International Limited, Sheffield, England
** Warsaw University of Technology, Poland
*** Sheffield University, England

Keywords: biaxial, non-proportional, damage, rainflow, plasticity

ABSTRACT: A method has been developed for making life predictions for engineering components subject to multiaxial loadings using the local strain approach. The method has been incorporated into a computer program which uses a Mròz-Garud [1,2] cyclic plasticity model and the Wang-Brown cycle counting and damage models [3,4]. The plasticity, rainflow cycle counting and damage models have been generalised to deal with any free-surface loading conditions. The program makes calculations based on strain gauge rosette measurements and its application is illustrated by calculations from three typical automotive components. Some interesting methods for visualising the analysis results are explored. In addition to life prediction, the approach also has applications in accelerated durability testing.

Introduction

Background

There is increasing pressure in the automotive industry to reduce the time taken to bring new designs to production, with typical development times coming down from around 5 years to around 2 years over the last decade. At the same time it is necessary for the vehicles developed to have low weight, high stiffness, good fuel efficiency, good ride and handling and good NVH properties (Noise Vibration and Harshness*) while maintaining adequate durability*. It is generally recognised that these objectives cannot be reasonably be met by developing the design through the testing and modification of a series of mechanical prototypes, because these methods are too time consuming and expensive. For this reason fatigue life prediction is now becoming an essential part of the development process for many vehicle manufacturers, and methods for reducing the time necessary for the essential fatigue tests are very important.

Fatigue life calculations tend to fall into two categories:

- Calculations made on the basis of calculated stresses and strains, for instance from Finite Element Analysis (FEA) [5-7].
- Calculations made on the basis of measured strains, typically from resistance strain gauges.

One of the most common approaches to fatigue analysis used in the automotive industry is the local strain approach. This paper is concerned with the application of multiaxial local strain methods to fatigue calculations of automotive components, based on strain gauge measurements.

Summary of method

Uniaxial methods for life prediction using the local strain approach have been in use for some time, having their roots in the work of Basquin [8] Manson [9] and Coffin [10,11], incorporating rainflow cycle counting and material memory [12] and Miners rule [13]. Such methods are available in commercial software products such as FATIMAS [14]. Within the well known limitations of these methods they work quite well for a variety of components where the local loading in the critical area is uniaxial or near-uniaxial. This class of components includes many that are subject to complex multiaxial loading environments [5,6]. However, there are many other components where a combination of loads and geometric effects generates local loadings which are proportional or non-proportional multiaxial. It was to deal with these cases that the methods and software discussed in the current paper were developed.

The life prediction process from measured strains can be divided into two steps. The first step is to determine the relationship between the measured strains and all the stress and strain components required for the damage calculation, through application of a cyclic plasticity model. The second step is to carry out cycle and damage accumulation. The current work addresses problems where the strains can be measured with a rosette, i.e. biaxial loading on a free surface. For these problems the process can be summarised by the flow chart in Figure 1:

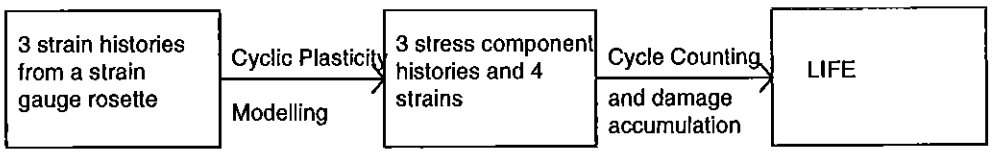

Fig.1 Outline of strain-based life prediction process.

The approach for calculations on the basis of elastic finite element analyses will be similar except that the input strains will be elastic strain components from the surface of the structure, and a notch correction procedure will be required in addition to the cyclic plasticity model to estimate the elastic-plastic stresses and strains [15].

The essential calculations made by the current system are as follows:

1. Take three strain channels from a strain gauge rosette and convert them to the components of strain ε_x, ε_y and ε_{xy} taking into account the transverse sensitivities of the gauge legs. The gauge co-ordinate system is defined by x parallel to gauge 1 and z as the outward surface normal.
2. Feed these 3 strain channels into the Mròz-Garud cyclic plasticity model, the outputs of which are the remaining non-zero strain component ε_z and the in-plane stresses σ_x, σ_y and σ_{xy}.
3. Process the resulting 7 components of stress and strain either by the conventional critical plane methods, or....
4. By multiaxial rainflow counting and then accumulating damage using the Wang-Brown methods.

These calculations are described in more detail in the following sections.

Cyclic Plasticity Modelling

The stresses and strains required by the damage models can be calculated if the relation between the equivalent plastic strain increment $\Delta\varepsilon_{eq}^{p}$ and the equivalent stress increment $\Delta\sigma_{eq}$ is known during the application of a given load increment. However, it is known that the current $\Delta\varepsilon_{eq}^{p} - \Delta\sigma_{eq}$ relation depends on the previous load path and therefore the plasticity model must deal with loading path dependent material constitutive behaviour.

Several models are available in the literature [1,2,16,17] of which the model proposed by Mròz [1] and recently modified by Garud [2] are the most popular. Mròz [1] has proposed that the uniaxial stress-strain material curve be represented by a set of plasticity surfaces in three dimensional stress space. In the case of a two dimensional stress state, the plasticity surfaces reduce to ellipses on the plane of principal stresses described by:

$$\sigma_{eq} = \sqrt{\sigma_1^{\,2} - \sigma_1 \cdot \sigma_2 + \sigma_2^{\,2}} \qquad (1)$$

and illustrated in Figure 2.

The load path dependent memory effects are modelled by prescribing a translation rule for the ellipses moving with respect to each other over distances given by the stress increments. It is also assumed that the ellipses move inside each other and they do not intersect. If the ellipses come in contact with one another they move together as a rigid body.

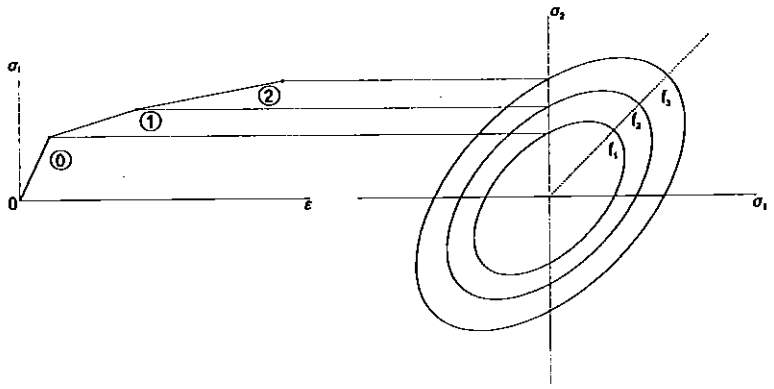

Fig.2 Linearisation of the material s-e curve and corresponding plasticity surfaces.

The translation rule proposed by Garud [2] avoids the intersection of the ellipses that could occur in some cases in the original Mròz [1] model. The Garud translation rule is illustrated in Figure 3 and can be described by a model consisting, for simplicity, of only two plastic surfaces (ellipses).

In order to predict material response due to the stress increment $d\sigma$, the following steps should be made:

1. Extend the stress increment $d\sigma$ to intersect the first external non-active plastic surface f_2 at point B_2
2. Connect point B_2 and the centre O_2 of the intersected plastic surface f_2
3. Find point B_1 on the active plastic surface f_1 by drawing a line parallel to the line O_2B_2 through the centre O_1 of the surface f_1
4. Connect the conjugate points B_1 and B_2 by the line B_1B_2
5. Translate the ellipse f_1 in the direction of B_1B_2 from point O_1' until the end of the vector $d\sigma$ lands on the moving ellipse f_1

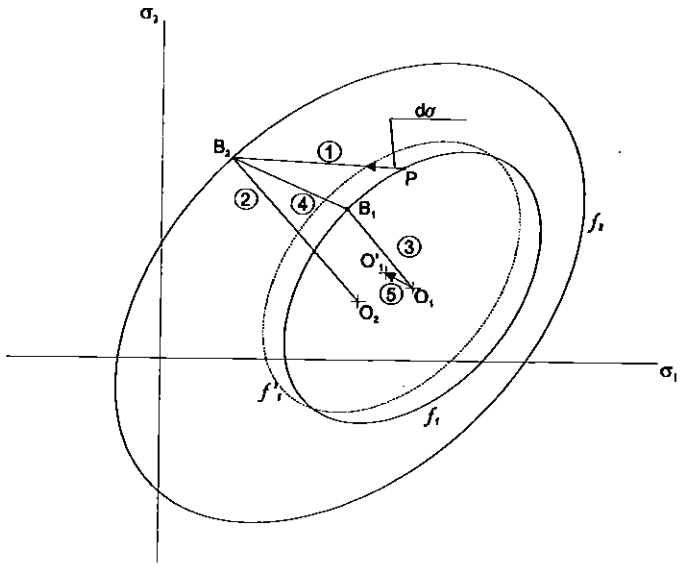

Fig.3 Geometrical interpretation of the Mròz-Garud incremental plasticity model.

The translation rule assures that the two ellipses are tangential with the common point B_1B_2 without intersecting each other. Two or more tangential ellipses translate as a rigid body and the largest moving ellipse (Figure 3) indicates the proper constitutive relation (linear segment) to be used for a given stress increment.

Multiaxial Rainflow Counting

Wang and Brown [18] proposed a multiaxial cycle counting method on the basis of strain hardening behaviour under non-proportional variable amplitude loading. Relative stresses and strains were introduced so that a pair of turning points define the start and end points of a reversal, where the equivalent relative strain rises monotonically to a peak value. Since plastic deformation generates the driving force for small fatigue cracks, hysteresis hardening provides a physical parameter for cycle counting, analogous to rainflow counting in the uniaxial case.

Each reversal commences with elastic unloading, which is followed by reloading and plastic strain hardening up to the next turning point. The most significant turning point occurs at the highest value of equivalent strain. This is illustrated at time 0 in Figure 4, which shows a repeating block of a combined tension/torsion non-proportional load history. The equivalent strain is defined as the von Mises strain.

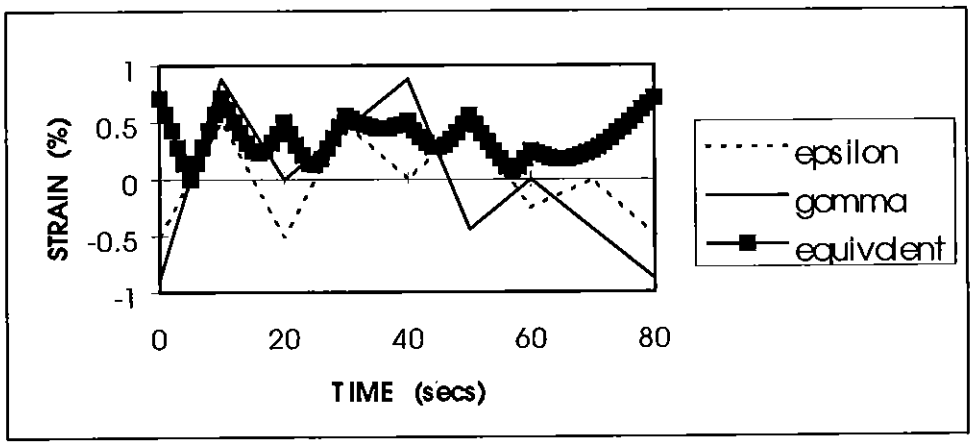

Fig.4 A variable amplitude non-proportional strain history, showing applied tensile (epsilon) and torsional (gamma) strains with the absolute equivalent strain.

The cycle counting method is illustrated by the following example. Starting from the most significant turning point, a graph is drawn for the loading block of relative equivalent strain, where relative strain $\varepsilon^{*}_{ij} = \varepsilon_{ij} - \varepsilon^{A}_{ij}$ represents the change of strain since time A. Figure 5 shows the relative equivalent strain, with respect to times 0, 10 and 20 seconds. Using the relative strain, a reversal can be defined starting from 0, up to the maximum value 10 seconds. To obtain the second reversal the relative strain is re-plotted starting from the next turning point where unloading commences (at 10 seconds), and the portions of the strain hardening curve for the reversal are selected by a traditional rainflow procedure [3]. The region of unloading and reloading within that reversal is counted in the next step.

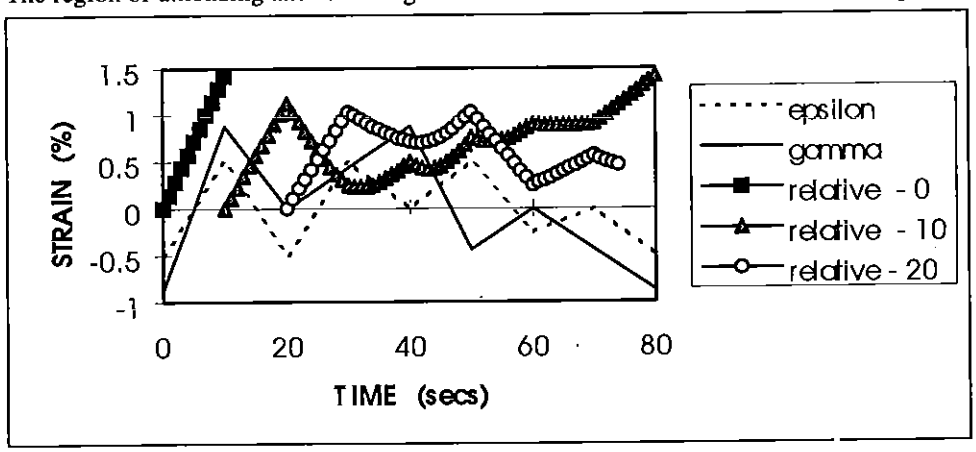

Fig.5 The variable amplitude history, showing relative equivalent strains plotted with respect to times 0, 10 and 20 seconds respectively.

Using the next turning point, relative strain is re-plotted with respect to 20 seconds for the subsequent continuous fragment of strain history, yielding the third reversal in Figure 5. This procedure is repeated for each turning point in chronological order, until every fragment of strain history has been counted.

Fatigue Damage Calculation

The counting method described above is independent of fatigue damage parameters, being based on hysteresis deformation behaviour. Being unrelated to material properties, it can be integrated with any multiaxial fatigue damage model. If the counted reversals are non-proportional, a fatigue damage parameter that accounts for non-proportional straining effects is required. The path-independent damage parameter proposed by Wang and Brown [19] has been shown to provide good correlation for several materials under proportional and non-proportional loading,

$$\hat{\varepsilon} \equiv \frac{\gamma_{max} + S.\delta\varepsilon_n}{1+\nu'+S(1-\nu')} = \frac{\sigma_f' - 2\sigma_{n,mean}}{E}(2N_f)^b + \varepsilon_f'(2N_f)^c \qquad (2)$$

where γ_{max} is the maximum shear strain amplitude on a critical plane (proportional or non-proportional), $\delta\varepsilon_n$ is the normal strain excursion between the two turning points of the maximum shear strain (that is the range of normal strain experienced on the maximum shear plane over the interval from start to end of the reversal), and $\sigma_{n,mean}$ is the mean stress normal to the maximum shear plane. The term S is a material constant determined from a multiaxial test (typically between 1 and 2 for Case A and around 0 for Case B) and ν' is the effective Poisson's ratio. The right hand side of the equation is the same as the uniaxial strain life equation, with a Morrow mean stress correction [20]. Mean stress is measured as the average of the maximum and minimum stress values over the reversal. The total damage induced by a loading history is calculated using Miner's rule [13].

Figure 6 is a plot of predicted life against experimental life for a variety of proportional and non-proportional tests on laboratory specimens, from Reference [4].

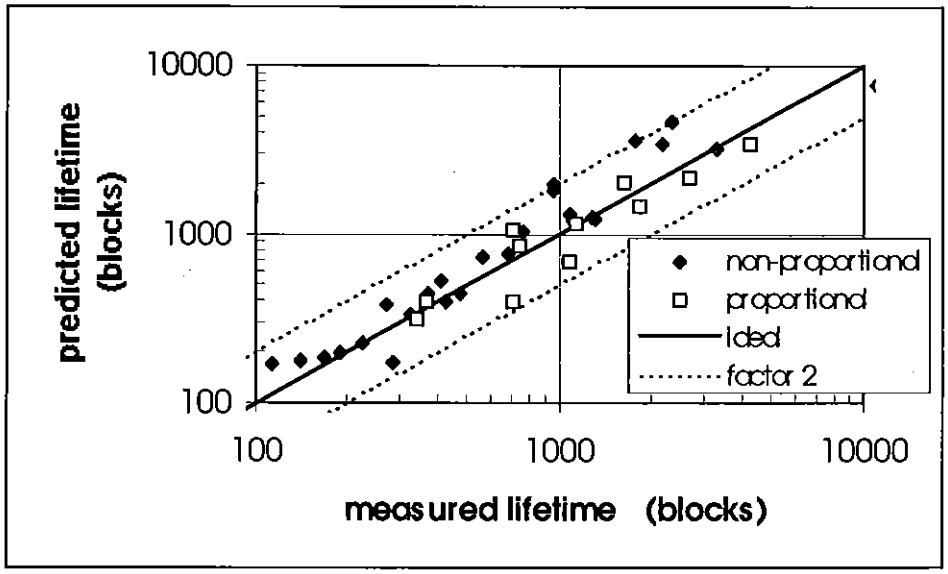

Fig.6 Comparison of experimental and predicted results for the Wang-Brown method.

The other multiaxial damage parameters considered in this paper are the more conventional critical plane parameters. In these methods, stresses and strains are resolved onto a particular plane, inclined at an angle $\theta = 90$ degrees (Case A) and/or $\theta = 45$ degrees (Case B) to the free surface. Cycle counting (uniaxial) and damage parameter calculation is carried out on the critical plane and the damage accumulated. The orientation ϕ of the projection of the normal to the damage plane is increased by 10 degree increments. The plane with the largest accumulated damage is said to be the critical plane. The models are:

1. Normal strain ($\theta = 90$ degrees only):

$$\frac{\Delta\varepsilon_n}{2} = \frac{\sigma'_f}{E}\left(2N_f\right)^b + \varepsilon'_f\left(2N_f\right)^c \tag{3}$$

ε_n is the strain amplitude normal to the critical plane. Otherwise this is the usual Coffin-Manson-Basquin equation.

2. Shear strain:

$$\frac{\Delta\gamma}{2} = \frac{(1+\nu_e)\sigma'_f}{E}\left(2N_f\right)^b + (1+\nu_p)\varepsilon'_f\left(2N_f\right)^c \tag{4}$$

3. Smith-Watson-Topper/Bannantine ($\theta = 90$ degrees only) [21]:

$$\frac{\Delta\varepsilon_n}{2}\cdot\sigma_{n,\max} = \frac{\sigma'^{\,2}_f}{E}\left(2N_f\right)^{2b} + \sigma'_f\cdot\varepsilon'_f\left(2N_f\right)^{b+c} \tag{5}$$

$\sigma_{n,max}$ is the maximum normal strain on the critical plane which occurs during each rainflow cycle. Otherwise this is the Smith-Topper-Watson method [22].

4. Fatemi-Socie [23]:

$$\frac{\Delta\gamma}{2}\left(1+n\frac{\sigma_{n,\max}}{\sigma_y}\right)=\frac{(1+\nu_e)}{E}\sigma'_f\left(2N_f\right)^b+\frac{n(1+\nu_e)\sigma'^{\,2}_f}{2E\sigma_y}\left(2N_f\right)^{2b}$$
$$+\left(1+\nu_p\right)\varepsilon'_f\left(2N_f\right)^c+\frac{n\left(1+\nu_p\right)\varepsilon'_f\sigma'_f}{2\sigma_y}\left(2N_f\right)^{b+c} \qquad (6)$$

Applications

The new program described in this paper may be used to predict the life of components and structures, to provide some help in design optimisation, and to assist in the design of efficient tests through fatigue editing. The main drawback of the program is that it is necessary to place a strain gauge rosette on the critical location or crack initiation site in order to get a reliable prediction. This is due to the fact that there is no simple transfer function between the measured strains at a non-critical location and the strains at a nearby critical location when the loading is non-proportional. For this reason, multiaxial fatigue life prediction is likely to be more useful when used in conjunction with Finite Element Analysis.

In this section, three applications of the multiaxial fatigue program will be described to illustrate the method.

Example 1: Fatigue calculations on an automotive wheel

This example is based on strain gauge measurements from an automotive wheel. The wheel was tested on a rig simulating the rotation of the wheel under load, and the strain gauge measurements were taken using a 45 degree rosette placed in the most critical location. This location was identified by previous stress analysis. A small section of the three strain gauge channels is illustrated in Figure 7.

The three channels of strain are more or less sinusoidal with a phase difference between them, indicating that the stress state is multiaxial and non-proportional. The two cycles shown above are taken from a longer history. The stress-strain state variations can be better understood qualitatively by looking at the behaviour of the principal stresses as illustrated in Figure 8, where it can be seen that the two principal stresses are almost in phase, but with slightly different amplitudes and means. Notice that the absolute maximum principal stress (the principal stress with the largest magnitude) "flips" between the

maximum and the minimum principals. Whenever it does this of course, the angle also flips through 90 degrees indicating that the state of stress has reached a condition where E.MAX and E.MIN are equal and opposite, i.e. pure shear. In fact the stress state behaviour can be summed up by saying that when the stress is at a maximum or minimum, the stress state is almost equibiaxial, and in between times it passes through a condition of pure shear where the stresses are lower. Between the two limits the principal stress axis rotates through 90 degrees, so that there is a complete rotation (180 degrees) per cycle.

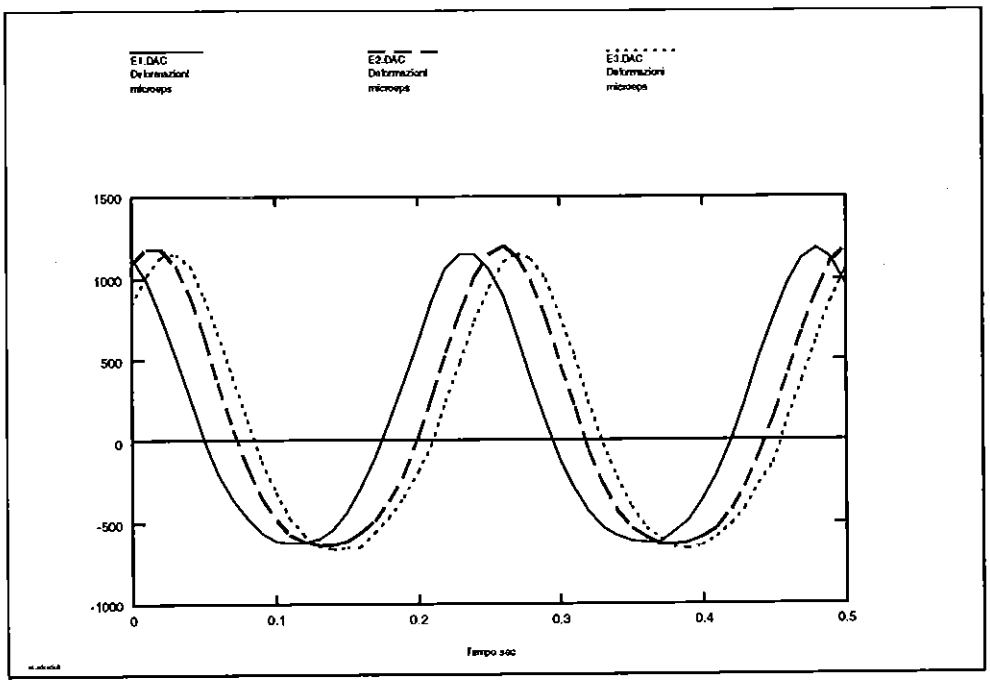

Fig.7 Section of strain measurements from wheel critical location.

Another way of looking at this data is to plot the biaxiality ratio (the ratio of the smaller in magnitude to the larger principal stress) and the orientation against the largest principal stress. This is shown in Figure 9 for 1 cycle.

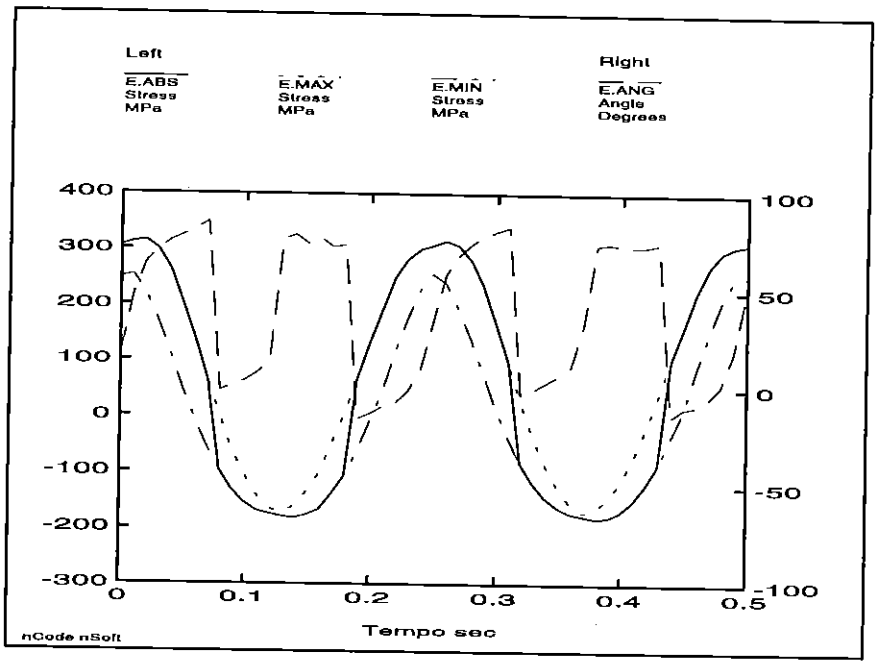

Fig.8 Plot of absolute maximum stress (E.ABS), maximum principal stress (E.MAX), minimum principal stress (E.MIN) and the angle of the absolute maximum principal stress to gauge 1 against time.

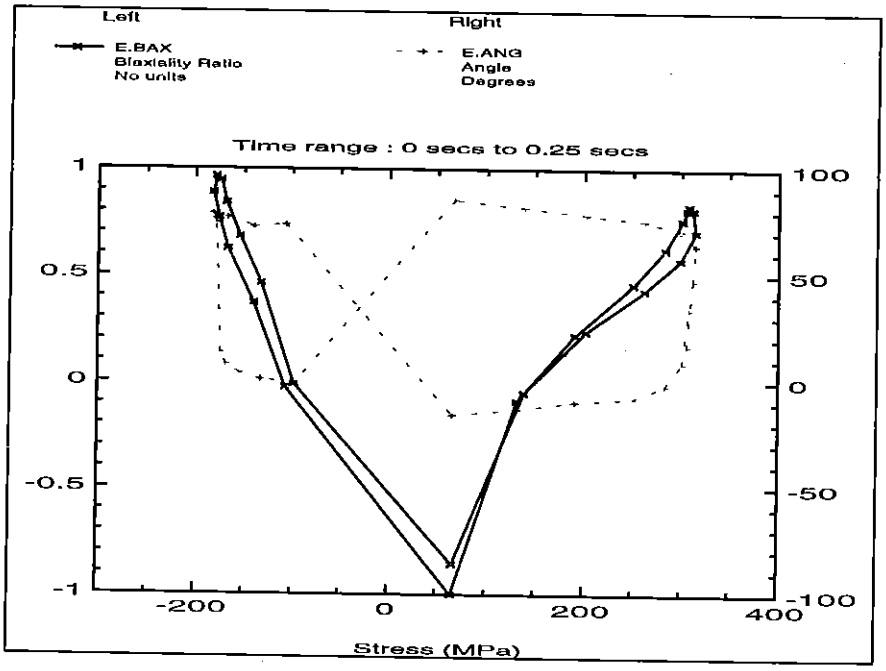

Fig.9 Plot of biaxiality ratio and angle against absolute maximum principal stress.

The results of analysis of the full loading history are given in Table 1, with the results of some other methods for comparison.

Table 1. Results of life calculations using various methods

Method	Life (Rotations)
Wang-Brown (S = 1 for Case A, 0 for Case B)	1.03×10^{6}
Wang-Brown + Mean (S = 1,0)	7.07×10^{5}
Normal Strain	5.54×10^{6}
Smith-Topper-Watson (Bannantine)	9.43×10^{5}
Shear Strain	5.95×10^{5}
Fatemi-Socie (n = 0.6)	5.17×10^{5}
Experiment	> 200000 (Test stopped with no failure)

These results are all very similar, with the notable exception of the normal strain method which is relatively non-conservative.

It is normal to view the accumulated rainflow cycles in an analysis in the form of a 3D histogram plot. Normally the axes are range-mean or max-min or from-to. With the Wang-Brown method, each cycle is characterised by shear strain range, normal strain range, mean normal stress, two angles θ and ϕ. The distribution of reversal numbers and damage may reasonably be visualised in relation to any two of these parameters. Figure 10 shows the distribution of reversals in relation to shear strain range and normal strain range. Another potentially useful way of viewing the results is in the form of a polar plot of damage, as shown in Figure 11. In this case there are only Case B damaging cycles, so there is only one curve on the plot.

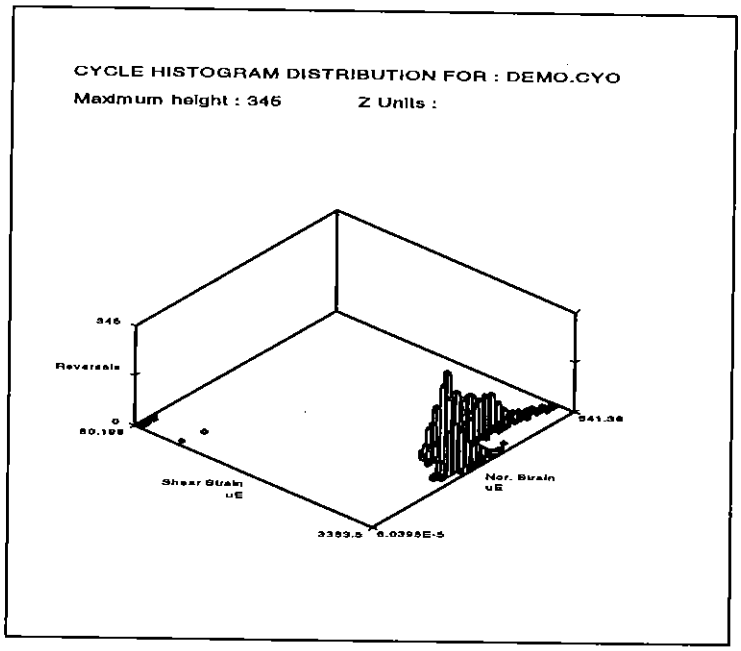

Fig.10 One representation of rainflow count.

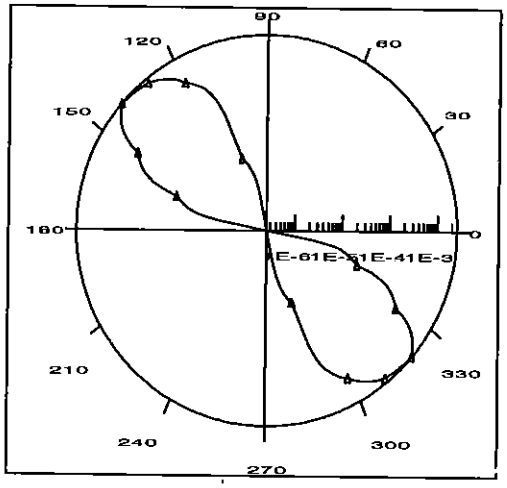

Fig.11 Polar plot of log(damage) against orientation ϕ.

Example 2: Fatigue life prediction of a steering rack mounting bracket

This example concerns a sign-off test which is carried out on a front suspension cross-member and steering rack assembly. The steering rack is mounted to the cross-member by means of two small brackets, which are fatigue-sensitive areas. The assembly is tested by fixing the cross-member and applying a constant amplitude, unidirectional load to the steering rack. The resulting stress state variations are illustrated in Figure 12.

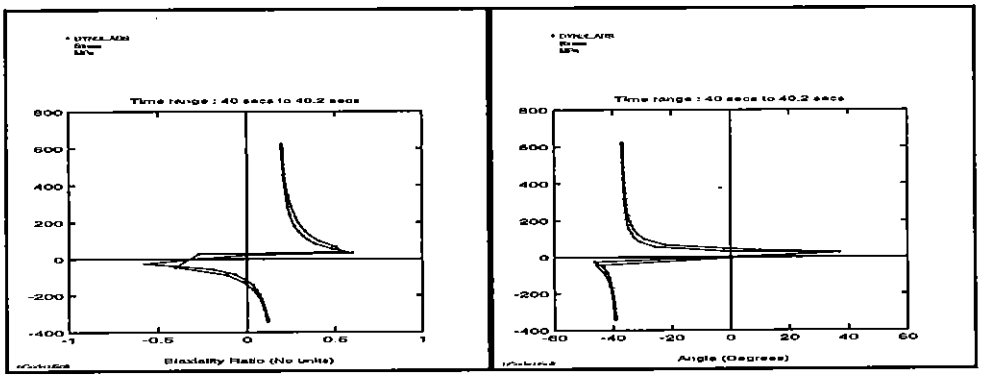

Fig.12 Plots of principal stress ratio (left) and principal axis orientation (right) plotted against absolute maximum principal stress.

These plots show that the single-axis loads applied generate locally a near-uniaxial, near proportional stress state. The results of analysis with the new program, assuming 99.9% certainty of survival (based on the calculated standard errors on the material parameters) are as given in Table 2:

Table 2. Fatigue life predictions on steering rack mounting bracket.

Method	Life (Repeats)
Wang-Brown (S = 1,0)	24
Wang-Brown + Mean (S = 1,0)	23
Normal Strain	33
Smith-Topper-Watson (Bannantine)	22
Shear Strain	23
Fatemi-Socie (n = 0.6)	23

Example 3: Fatigue editing on an off-road vehicle rear axle

This example illustrates how the new program can be used to reduce testing times through multiaxial, multi-channel fatigue editing of simulation test rig drive files. The component in question is a rear axle from an off-road vehicle. The axle is instrumented with three strain gauge rosettes close to critical locations, and analysis of the measurements from all three strain gauge rosettes show that the loading is non-proportional. It is desired to reduce the testing time by editing the rig drive signals while retaining all the sections of the original sections that cause significant damage. This was carried out using a simple editing procedure.

One of the outputs of the life prediction program is a time correlated damage file, essentially a time history of damage. This file is a record of the damage accumulated, with damage for each reversal being distributed between the opening and closing point of each reversal. The signal is divided up into a number of equally spaced windows, and the least damaging are discarded until a certain percentage of damage is retained, in this example 95% was retained. The time slices to be retained are compared across the three channels with a logical OR operation and all the resulting windows are retained. The resulting edit vector can be used to edit the rig drive signals, inserting suitable joining functions for continuity. It is also important to edit the strain signals and recalculate the life in order to check the likely effect of editing on the fatigue damage. This is important because of the possibility of reversals starting in one window and ending in another, and also because in multiaxial loading the loading path is important as well as the peaks. In some cases, editing the signals may actually cause a slight increase in fatigue damage. This is why methods such as described in Reference [24] are not really suitable for non-proportional loadings, because they do not retain the important sections of the loading path. The results of the analysis described are summarised in Table 3 and the original and edited strain signals for Gauge 1 are illustrated in Figure 13.

Table 3. Summary of fatigue editing results.

Gauge Number	Original Signal Predicted Life (repeats)	Edited Signal Predicted Life (repeats)	Actual Damage Retained	Data Reduction Factor
1	13866	14079	98.5	8.25
2	29770	30188	98.6	8.25
3	53200	53800	98.8	8.25

The advantages of this method are that it retains both the most important sections of loading path, and the essential frequency content of the loading, essential for components with dynamic behaviour.

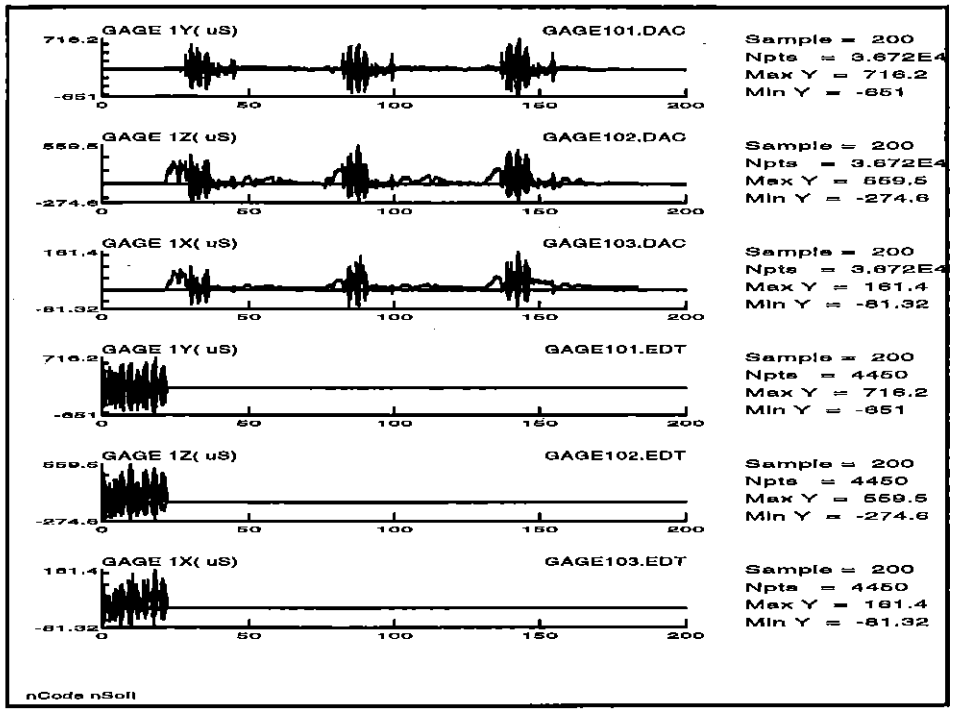

Fig.13 Strain signals before and after editing.

Concluding remarks

1. A new computer program has been written which incorporates a Mròz-Garud [1,2] cyclic plasticity model, together with a generalised form of the Wang-Brown [3,4] multiaxial rainflow and damage accumulation procedures. The program also incorporates a variety of other critical plane damage models. The program requires measured strains from strain gauge rosettes as input, together with uniaxial cyclic material properties. The software has a graphical user interface and various post-processing options.
2. The software has been applied to strain measurements from three different components, including one with an interesting Case B biaxial non-proportional loading.
3. The software can handle general non-proportional biaxial loadings.
4. A variety of multiaxial damage parameters have been applied and compared.
5. The approach described here would benefit from more validation within an industrial context, and will also benefit from being extended to interface to finite element analysis. This is planned for the near future.

References

(1) MRÒZ Z., (1967), On the Description of Anisotropic Work Hardening, Journal of Mechanics and Physics of Solids, vol. 15, pp. 163-175

(2) GARUD Y. S., (1981), A New Approach to the Evaluation of Fatigue under Multiaxial Loading, Journal of Engineering Materials and Technology, vol. 103, pp. 118-125

(3) WANG C. H. and BROWN M. W., (1996), Life Prediction Techniques for Variable Amplitude Multiaxial Fatigue - Part 1: Theories, Journal of Engineering Materials and Technology, vol. 118, pp. 367-370

(4) WANG C. H. and BROWN M. W., (1996), Life Prediction Techniques for Variable Amplitude Multiaxial Fatigue - Part 2: Comparison with Experimental Results, Journal of Engineering Materials and Technology, vol. 118, pp. 371-374

(5) HEYES P. J., MILSTED M. G. and DAKIN J., (1996), Multiaxial Fatigue Assessment of Automotive Chassis Components on the basis of Finite-Element Models, Multiaxial Fatigue and Design, ESIS 21 (Edited by A. Pineau, G. Cailletaud and T. C. Lindley) MEP London, pp. 461-475

(6) HEYES P., DAKIN J. and ST.JOHN C., (1995), The Assessment and Use of Linear Static FE Stress Analyses for Durability Calculations, Proceedings of the Ninth International Conference on Vehicle Structural Mechanics and CAE, pp. 189-199

(7) HEYES P. and FERMÉR M., (1996), A Program for the Fatigue Analysis of Automotive Spot-Welds Based on Finite Element Calculations, Proceedings of the Symposium on International Automotive Technology, SAE Technical Paper 962507

(8) BASQUIN O. H., (1910), The Exponential Law of Endurance Tests, Proceedings of the American Society for Testing Materials, vol. 10, pp. 625-630

(9) MANSON S. S., (1953), Behaviour of Materials under Conditions of Thermal Stress, Heat Transfer Symposium, University of Michigan Engineering Research Institute, pp. 9-75

(10) COFFIN L. F., (1954), The Problem of Thermal Stress Fatigue in Austenitic Steels at Elevated Temperatures, ASTM STP No. 165, p.31

(11) COFFIN L. F., (1954), A Study of the Effects of Cyclic Thermal Stresses on a Ductile Metal, Trans. American Society for Testing and Materials, vol. 76, pp. 931-950

(12) MATSUISHI M. and ENDO T., (1968), Fatigue of Metals Subjected to Varying Stress, Presented to Kyushu District Meeting, JSME.

(13) MINER M. A., (1945), Cumulative Damage in Fatigue, Journal of Applied Mechanics, vol. 12, pp. A159-A164

(14) nCode International Ltd., (1997), nSoft-E FATIMAS software manual

(15) GLINKA G. and BUCZYNSKI A., (1997), Elastic-Plastic Stress-Strain Analysis of Notches under Non-Proportional Cyclic Loading Paths, Proceedings of the 5th International Conference on Biaxial/Multiaxial Fatigue and Fracture, Krakow, Poland

(16) CHU C. C., (1989), A Three-Dimensional Model of Anisotropic Hardening in Metals and its Application to the Analysis of Sheet Metal Formability, Journal of Mechanics and Physics of Solids, vol. 22, no. 3, pp. 197-212

(17) ARMSTRONG P. J. and FREDERIC C. O., (1966), A Mathematical Representation of the Multiaxial Bauschinger Effect, CEGB Report RD/B/M731, Berkeley Nuclear Laboratories

(18) WANG C. H. and BROWN M. W., (1993), Inelastic Deformation and Fatigue under Complex Loading, Proceedings of the 12th International Conference on Structural Mechanics in Reactor Technology, vol. L, pp. 159-170

(19) WANG C. H. and BROWN M. W., (1993), A Path-Independent Parameter for Fatigue under Proportional and Non-Proportional Loading, Fatigue and Fracture of Engineering Materials and Structures, vol. 16, pp. 1285-1298

(20) BROWN M. W., SUKER D. K. and WANG C. H., (1996), An Analysis of Mean Stress in Multiaxial Random Fatigue, Fatigue and Fracture of Engineering Materials and Structures, vol. 19, no. 2/3, pp. 323-333

(21) BANNANTINE J. A., (1989), A Variable Amplitude Multiaxial Fatigue Life Prediction Method, PhD thesis, University of Illinois at Urbana-Champaign

(22) SMITH K. N., WATSON P. and TOPPER T. H., (1970), A Stress-Strain function for the Fatigue of Metals, Journal of Materials, vol. 5, no. 4, pp. 767-778

(23) FATEMI A. and SOCIE D. F., (1988), A Critical Plane Approach to Multiaxial Fatigue Damage Including Out-of-Phase Loading, Fatigue and Fracture of Engineering Materials and Structures, vol. 11, no. 3, pp.149-165

(24) DREßLER K., KÖTTGEN V. B. and KÖTZLE H., (1995), Tools for Fatigue Evaluation of Non-Proportional Loading, Proceedings of Fatigue Design 1995 (Edited by Gary Marquis and Jussi Solin), vol. 1, pp. 261-277

Acknowledgements: The authors are grateful for financial support from Ford Motor Company and the Department of Trade and Industry. We would also like to thank Prof. Gregory Glinka for his support and Fiat Auto, The Ford Motor Company and Jaguar Cars for providing information about the applications.